

Synthesis, Characterization and Role of Zinc Oxide Nanoparticles in Wheat (*Triticum indicum*) Seeds Germination

Tajnees Pirzada^{a*}, Weenghar Ali Chandio^a, Mir Munsif Ali Talpur^a, Abdul Majid Ansari^b and Fayaz Hussain Kanhar^a

^aInstitute of Chemistry, Shah Abdul Latif University, Khairpur, Sindh, Pakistan

^bDepartment of Biochemistry, Shah Abdul Latif University, Khairpur, Sindh, Pakistan

(received March 02, 2020; revised December 26, 2020; accepted January 25, 2021)

Abstract. The current research was undertaken to examine the zinc oxide nanoparticles (ZnO NPs) effects on wheat (*Triticum indicum*) seeds germination and development. ZnO NPs were synthesized using co-precipitation method and their role in wheat seeds germination was determined. Prepared ZnO NPs were characterized using XRD, SEM, FTIR, UV-Visible spectroscopy. The particles crystallite determined by using XRD. SEM images showed size in range of 20 nm - 25 nm diameter. *In vitro* experiments of ZnO NPs at different concentrations (5 ppm, 10 ppm, 15 ppm and 20 ppm) were conducted to see the effects on germination of wheat seeds. The mortality rate of germinated wheat was decreased from 34% to 15% for control and 20 ppm samples of ZnO NPs, respectively. The root length was found to be increased from 82 mm, 88 mm, 89 mm and 90 mm for 5 ppm, 10 ppm, 15 ppm and 20 ppm respectively. Fresh weight was also increased from 2 g to 2.36 g, for 5 g to 20 g, respectively. All experiments were carried in triplicate. Growth of the plant i.e. the length of root and shoot enlarged significantly at 20 ppm. This study confirmed that crystallite ZnO NPs could be an alternate to available fertilizers.

Keywords: ZnO NPs, XRD, SEM, FTIR, UV-Visible, wheat germination

Introduction

Nanotechnology is the synthesis of materials at nanoscale (up to 100 nm in any direction) using top-down or bottom-up approaches. Due to the higher surface to volume ratio, nanoscale materials have pronounced effects on strength, weight and chemical reactivity due to their increased surface to volume ratio. Such materials are already in use of analytical instruments, systems for the drug delivery and production of green energy also for such other materials (Lee and Yong, 2013). Due to bio-compatibility and catalytic activity ZnO NPs are employed as a heterogeneous catalyst (Yusan *et al.*, 2016). Nanotechnology in the field of agriculture consisting of nano fertilizer and nano pesticides provides increased nutrients. The contaminants are removed from soil and water, when ZnO NPs replenish into the soil (Prasad *et al.*, 2017).

Preparation of ZnO NPs in controlled and precise way reveals the fate of transformed materials (Albrecht *et al.*, 2006). There are various methods for the synthesis of nano materials such as physico-chemical in which pressure, energy, temperature and toxic solvents and in biological methods are included. Nano materials synthesized from naturally occurring microorganisms

possess vast potential in natural products. In spite of the toxicity and adverse effects of metal nanoparticles, NPs can be successfully utilized by managing their application conditions and parameters (Rawashdeh *et al.*, 2020). Various parts of plants like bark, root, leaves, fruit, flowers and latex are considered to be common sources for the synthesis of nanoparticles by using chemical and physical methods having multi-dimensions, varies in size, shape and dispersion (Prasad *et al.*, 2017; Rosi and Mirkin, 2005).

ZnO NPs can be applied in industries for the production of cosmetics, coatings, dye-sensitized solar, sensors and medicines as well as antibacterial properties (Mishra and Adelung, 2018; Dhobale *et al.*, 2008) and play vital role as growth factor for plant as mentioned in research.

ZnO NPs being a small three dimensional structures lead to control the agricultural process. Literature reveals that the use of NPs for treating seeds is more efficient and advantageous over traditional treatment utilizing fertilizers in terms of plant yield and quality (Pereira *et al.*, 2017). In agriculture limited availability of natural resources is still the point to of concerns. Nano scale nutrient enhances the fertilization to provide nutrient in extended manners. However, to the best of our knowledge, applications of ZnO NPs on seedling

*Author for correspondence; E-mail: tajnees@yahoo.com

development of wheat or seed germination profile of wheat of have not been reported.

In this study, synthesized ZnO NPs were characterized using variety of physico chemical techniques such as, SEM, XRD, FTIR spectroscopy and UV-Visible spectroscopy. In addition, their effect on seedling development and germination profile was investigated. This study could be helpful for the implementation of nano-technology for the betterment of agriculture.

Materials and Methods

ZnO NPs synthesis. ZnO NPs were prepared by applying the co-precipitation method, using potassium hydroxide (KOH) and zinc acetate. The method of synthesis was modified from (Rekha *et al.*, 2010) after modification of several parameters. Finally, 1.48 g of salt commercially available zinc acetate (HmBG Chemicals) dissolved in 63 mL of absolute ethyl alcohol (HmBG Chemicals) in a 250 mL conical flask and heated up to 60 °C with continuous shaking and 0.74 g of KOH (VWR Amresco, US) were also dissolved separately in 33 mL of absolute ethyl alcohol under similar condition. Subsequently, KOH was added into zinc acetate slowly at 60 °C with constant stirring. The solution was left for 3 h under continuous stirring, white precipitates of ZnO NPs were obtained and collected by centrifugation for 10 min at 4000 rpm, and then washed with de-ionised water several times. The white precipitates were finally dried in oven at 60 °C.

Characterization of ZnO nanoparticles (Instrumentation). Various techniques XRD, SEM, FTIR and UV-Vis spectroscopy were employed to characterize the synthesized ZnO NPs. Crystal structure, primary crystal, morphological features especially the size and shape of ZnO NPs.

Powder X-ray diffraction (XRD). Powder XRD patterns of samples were observed by Diffractometer system (XPRT-PRO). The specification for instrumentation were followed for each sample i.e. Cu; voltage/current, 10 kV/50 mA; scan speed, 4°/min, 1.5 nm wavelength, 2 Θ ranges from 10-80 Θ . The mean crystallite size was less than 20 nm of the ZnO NPs were estimated using Debye-Sherrer equation (eq. 1).

$$D = k\lambda / \beta \cos \theta \dots\dots\dots\text{eq. 1}$$

whereas:

k is Sherrer constant, β is full width at half maximum, λ denotes wavelength and θ reflects the angle of Bragg's Diffraction.

Scanning electron microscopy (SEM). SEM images of the samples were obtained by Joel JSM-840 scanning electron microscope with a 10 kV accelerating voltage by gold coating the surface of samples for SEM was made conductive by applying electricity in sputtering device.

UV-Visible spectroscopy. By Shimadzu, UV-Visible spectrophotometer, the spectra of sample solutions were observed by recording the spectra in a 1 cm quartz cuvette in the wavelength range 200-800 nm.

Fourier transform infra red spectroscopy (FTIR). The FTIR spectra of samples were recorded on SENSIR. The samples (2 mg) were powdered in a clean glass pestle and mortar and scans were recorded from 1500-500/cm.

Application of ZnO NPs on seed germination. Untreated and unprocessed wheat samples were obtained from Sadiqabad, Pakistan. The weight of 100 seeds (grains) was weighed as 3.95 g. Seed germination on cellulose filter paper was performed according to method described by Kaur and Singh (2006) in the transparent trays in presence of light. Distilled water washed seeds of wheat plant were placed on filter paper, ten seeds per plate in approximately 1 cm distance in a series of Petri dishes. Prior distilled water was added to filter papers for humidification. 2 mL of treatment solution of ZnO NPs, containing 5, 10, 15 and 20 ppm were spread thoroughly on to filter paper. Seed were kept humid and seed germination was recorded after interval of 24 h. After 15 days germinated seedling were harvested and mortality rate, root elongation, seed germination (seeds with roots longer than 5 mm were considered geminated), root length, shoot length, root and shoot fresh weight and dry weight were recorded. Dry weight was achieved after the drying seedlings in oven at 60 °C for 48 h (Kibbey and Strevett, 2019). Three replicates were performed for each test along positive and negative controls (soil and water, respectively). The germination percentage in each test was measured by root length with a ruler on filter paper. The root elongation and seed germination were calculated according to equation (2 and 3, respectively), while, percentage mortality was calculated using equation 4.

$$\text{Root elongation} = ((\text{Mean root length of test sample}) / (\text{Mean root length of control})) \times 100 \dots\dots\dots\text{eq. 2}$$

$$\text{Seed germination} = ((\text{Seed germination of test sample}) / (\text{Seed germination of control})) \times 100 \dots\dots\dots\text{eq. 3}$$

$$\text{Mortality} = ((\text{Seed mortality of test sample})/(\text{Seed mortality of control})) \times 100 \dots\dots\dots \text{eq. 4}$$

Results and Discussion

XRD patterns of ZnO NPs. The size of crystallite and purity of synthesized ZnO NPs were resolved by Diffractometer. From the XRD pattern of ZnO NPs, presented in Fig. 1, it was noticed that all the peaks are well matched with the wurtzite structure standard as predicted in JCPDS Card No. 36-1451 (Fortunato *et al.*, 2009; Özgür *et al.*, 2009). Peaks at diffraction angles (2θ) of 24°, 31°, 32°, 34°, 37°, 41°, 44°, 46°, 54°, 58°, 61° and 64° correlated to the reflection from (100), (002), (101), (102), (110), (103), (200), (112) and (201) the hexagonal crystal planes of wurtzite ZnO NPs structures (Yang *et al.*, 2006).

Further, the mean crystallite size was less than 20 nm of the ZnO NPs were estimated using Debye-Sherrer equation (eq. 1). In XRD spectra, all the diffraction peaks of the synthesized nanoparticles showed sharp peak intensities, indicating crystallinity ZnO NPs.

SEM studies. Due to the very narrow electron beam, micrographs of SEM are useful for understanding the surface structure of sample possessing a large depth of field appearing in a characteristic three-dimensional form. However, the sub-microscopic images i.e. micrographs of ZnO NPs for this study are shown in Fig. 2 with magnification of 5000X and 10 KV, respectively.

The aggregates of ZnO NPs are clearly indicated in micrographs and the size of these aggregates was nearly

similar. Further, images showed large agglomerates or clusters of ZnO NPs. Surface of these aggregates were rough in nature that may be attributed to the nanorods of ZnO. A number of researchers have reported similar magnification images and showed homogeneous shape and size for ZnO NPs (Zak *et al.*, 2011).

UV-Visible spectroscopy. The absorption spectroscopy has been widely used technique for the determination of optical properties of nanosized particles. The role of nanoparticles is important in changing the entire properties of materials. Thus, size evolution of semiconducting nanoparticles becomes very essential to investigate the properties of the materials. The UV-Visible spectra of ZnO NPs is shown in Fig. 3 which exhibits a strong absorption band at about 357 nm attributed to the ZnO nanoparticles and small band at 258 nm appeared much above the band gap wavelength of 357 nm. A significant absorption of ZnO NPs gives the idea of the monodispersed nature of the nanoparticle distribution which was also confirmed by SEM analysis

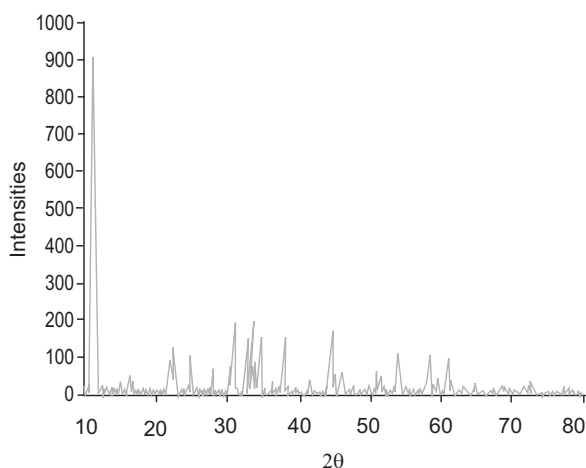


Fig. 1. XRD pattern of ZnO NPs.

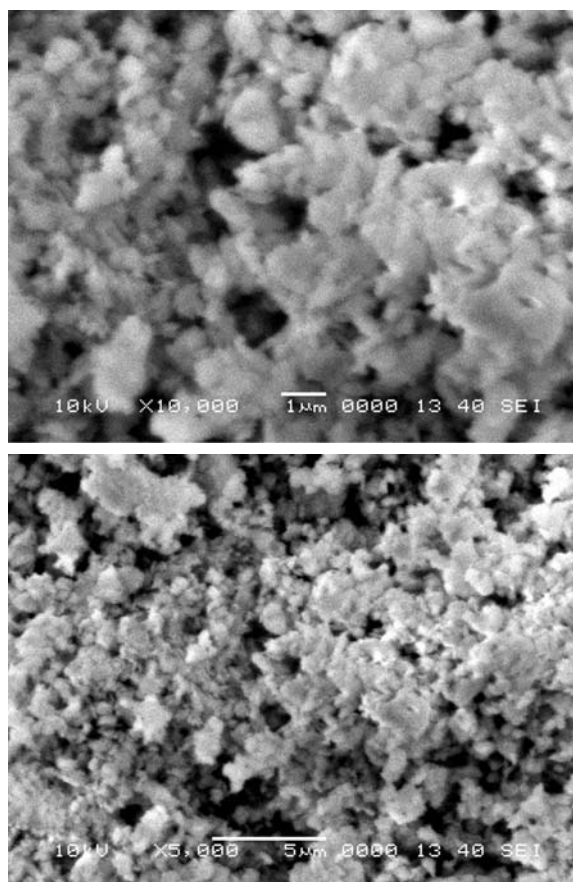


Fig. 2. SEM micrographs of ZnO NPs.

(Arote *et al.*, 2019; Lavand and Malghe, 2018; Salavati-Niasari *et al.*, 2011; Zak *et al.*, 2011).

Fourier transform infrared spectroscopy (FT-IR).

The FTIR spectrum was observed in the range of 1500-500/cm are presented in Fig. 4, shows predominant peaks at 920 and 700/cm. In spectrum of synthesized ZnO NPs appearance of characterized strong peak at 700/cm indicates the successful synthesis of ZnO NPs as shown in Fig 4. The peak 1458/cm are assigned to bending vibrational mode of water molecules and peak positioned at 920/cm corresponds to degenerate symmetric stretching mode of acetate ions.

Application of synthesized ZnO NPs on germination of wheat. ZnO NPs were applied to the seeds of wheat

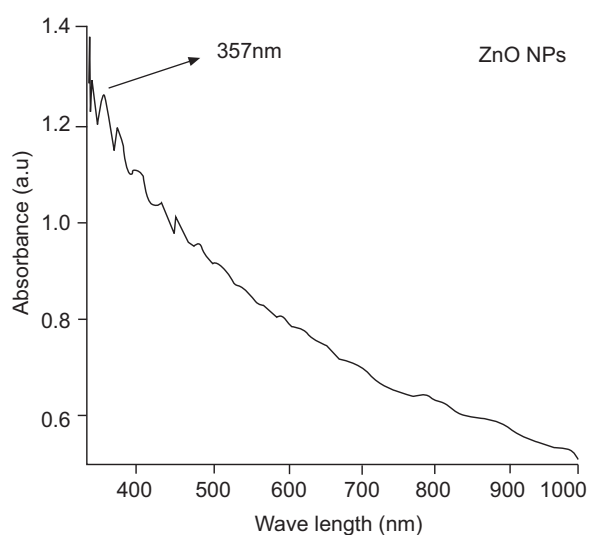


Fig. 3. UV-Visible spectra of ZnO NPs.

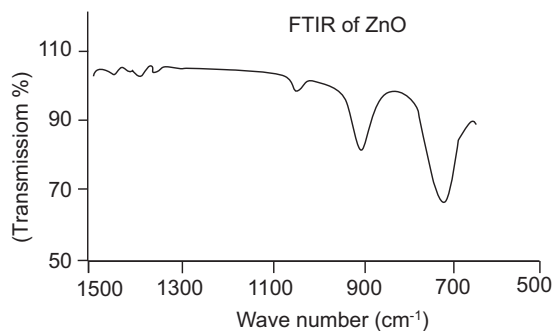


Fig. 4. FTIR spectra (1500-500/cm range) of synthesized ZnO NPs.

plant in order to examine the effectiveness of applying NPs in the enhancing plant growth and development. More pronounced results were obtained by ZnO NPs when compared with Zn. It is reported by Awasthi *et al.* (2017) that growth decreases with increased concentration of Zn.

Germination. Germination of seed started from the fourth day after cultivation and recorded on the same day continued for 14 days as described by (Seyedi *et al.*, 2002). Germination and seedling of wheat decrease with increasing concentration as shown in Fig. 5. Growth of plant was found highest (76.6%) by applying continuously 5 ppm solution of prepared ZnO NPs,

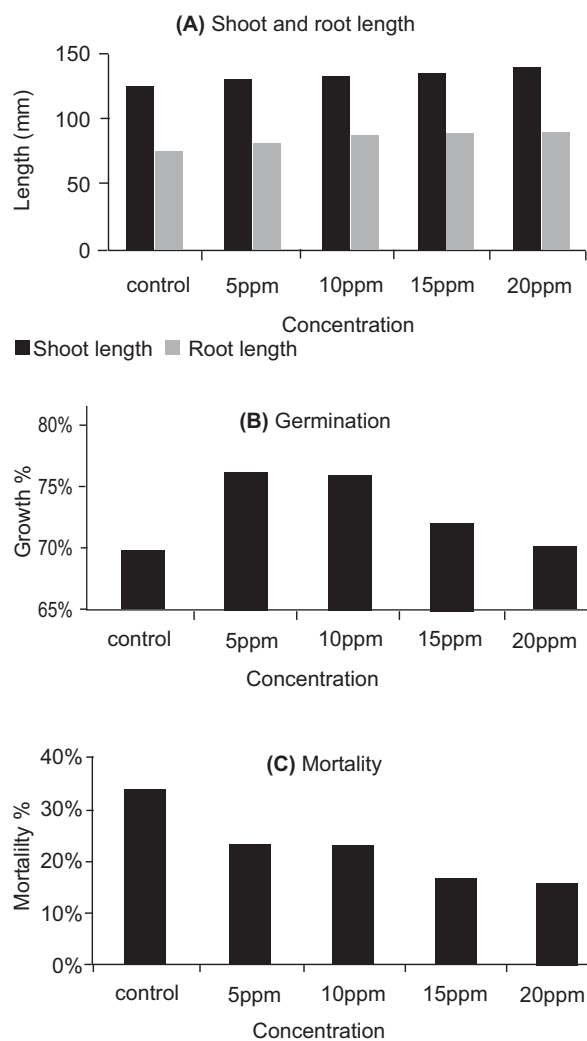


Fig. 5. Effect of synthesized ZnO NPs on germination of wheat seed (A) Shoot and root length (B) Germination (C) Mortality.

whereas minimum growth (70%) recorded with control (DD water). It has been reported by several workers that seed treatment with ZnO NPs helps in the germination process, such as breaking of dormancy, hydrolysis or metabolization of inhibitors and enzyme activation (Mondal and Bose, 2019; Rizwan *et al.*, 2019).

Mortality. The mortality percentage is presented in Fig. 5. Mortality is considered to be reverse of germination. Highest transience of plant (34%) observed with control and lowest (15%) were recorded with 20 ppm ZnO NPs solution.

Seedling growth. Shoot and root length. The shoot and root of seedlings were measured by ruler after ten days. The highest shoot Length of 140.83 mm was observed with the application of 20 ppm ZnO NPs which decreased upto 126.2 mm under control (see Fig. 5). The shoot length significantly observed increasing with concentration of ZnO NPs, whereas the root length (90.3 mm) found increasing with concentration of ZnO NPs and lowest growth recorded under control. Majority of root shoot length differences appeared after the long period. Similar findings were reported in literature where, ZnO NPs concentration effects on the root and shoot length of other plants precursor activity of Zn, especially ZnO NPs in auxin production (Awasthi *et al.*, 2017).

Fresh and dry weight. Seedling fresh and dry weights were recorded by a digital scale (XPR Microbalance, Metler, UK). The wheat plant fresh as well dry weight increasing with concentration of ZnO NPs 5-20 ppm. At 20 ppm highest fresh and dry weight of seedlings 2.36 and 1.5 g were calculated. However, the lowest (1.6 and 0.9 g) were observed under control (Table 1).

Table 1. Effect of different concentration ZnO NPs on fresh and dry weight of wheat in petri dishes

Parameters	Water cont;	5ppm	10ppm	15ppm	20ppm
Fresh weight /g	1.6	2	2.1	2.1	2.36
Dry weight /g	0.9	1.1	1.2	1.26	1.5

Conclusion

ZnO NPs having size 20-25 nm were synthesized by Co precipitation method, then characterized by XRD,

SEM, FTIR and UV-Visible spectroscopy. In UV-Visible spectra strong band at 357 nm and appearance of characterized strong peak in FTIR at 700/cm confirmed the successful synthesis of ZnO NPs. The effect of ZnO NPs was observed on the wheat seed germination and its growth. Different (5-20 ppm) concentrations of ZnO NPs were applied and it was found that at 5ppm ZnO NPs showed highest positive effects on seedling growth over control on seed germination with lowest mortality rate under control. However, the root and shoot growth, dry and fresh weight increased with higher concentration of ZnO NPs in the treatment.

Conflict of Interest. There is no conflict of interest among authors.

References

- Albrecht, M.A., Evans, C.W., Raston, C.L. 2006. Green chemistry and the health implications of nanoparticles. *Green Chemistry*, **8**: 417-432. <https://doi.org/10.1039/B517131H>
- Arrote, S.A., Pathan, A.S., Hase, Y.V., Bardapurkar, P.P., Gapale, D.L., Palve, B.M. 2019. Investigations on synthesis, characterization and humidity sensing properties of ZnO and ZnO-ZrO₂ composite nanoparticles prepared by ultrasonic assisted wet chemical method. *Ultrasonics Sonochemistry*, **55**: 313-321. <https://doi.org/10.1016/j.ultsonch.2019.01.012>
- Awasthi, A., Bansal, S., Jangir, L.K., Awasthi, G., Awasthi, K.K., Awasthi, K. 2017. Effect of ZnO nanoparticles on germination of *Triticum aestivum* seeds. In *Macromolecular Symposia*, **376**: 1022-1360. <https://doi.org/10.1002/masy.201700043>
- Dhobale, S., Thite, T., Laware, S.L., Rode, C.V., Koppikar, S.J., Ghanekar, R.K., Kale, S.N. 2008. Zinc oxide nanoparticles as novel alpha-amylase inhibitors. *Journal of Applied Physics*, **104**: 904-909. <https://doi.org/10.1063/1.3009317>
- Fortunato, E., Gonçalves, A., Pimentel, A., Barquinha, P., Gonçalves, G., Pereira, L., Martins, R. 2009. Zinc oxide, a multifunctional material: from material to device applications. *Applied Physics A*, **96**: 197-205. <https://doi.org/10.1007/s00339-009-5086-5>
- Kaur, M., Singh, N. 2006. Relationships between selected properties of seeds, flours and starches from different chickpea cultivars. *International Journal of Food Properties*, **9**: 597-608. <https://doi.org/10.1080/10942910600853774>
- Kibbey, T.C., Strevett, K.A. 2019. The effect of

- nanoparticles on soil and rhizosphere bacteria and plant growth in lettuce seedlings. *Chemosphere*, **221**: 703-707. <https://doi.org/10.1016/j.chemosphere.2019.01.091>
- Lavand, A.B., Malghe, Y.S. 2018. Synthesis, characterization and visible light photocatalytic activity of carbon and iron modified ZnO. *Journal of King Saud University-Science*, **30**: 65-74. <https://doi.org/10.1016/j.jksus.2016.08.009>
- Lee, D., Yong, K. 2013. Non-vacuum deposition of CIGS absorber films for low-cost thin film solar cells. *Korean Journal of Chemical Engineering*, **30**: 1347-1358. <https://doi.org/10.1007/s11814013-0101-0>
- Mishra, Y.K., Adelung, R. 2018. ZnO tetrapod materials for functional applications. *Materials Today*, **21**: 631-651. <https://doi.org/10.1016/j.mattod.2017.11.003>
- Mondal, S., Bose, B. 2019. Impact of micronutrient seed priming on germination, growth, development, nutritional status and yield aspects of plants. *Journal of Plant Nutrition*, **42**: 2577-2599. <https://doi.org/10.1080/01904167.2019.1655032>
- Özgür, Ü., Alivov, Y., Morkoç, H., 2009. Microwave ferrites, part 1: fundamental properties. *Journal of Materials Science: Materials in Electronics*, **20**: 789-834. <https://doi.org/10.1007/s10854-009-9923-2>
- Pereira, A.E.S., Sandoval-Herrera, I.E., Zavala-Betancourt, S.A., Oliveira, H.C., Ledezma-Pérez, A.S., Romero, J., Fraceto, L.F. 2017. γ -Polyglutamic acid/chitosan nanoparticles for the plant growth regulator gibberellic acid: characterization and evaluation of biological activity. *Carbohydrate Polymers*, **157**: 1862-1873. <https://doi.org/10.1016/j.carbpol.2016.11.073>
- Prasad, R., Bhattacharyya, A., Nguyen, Q.D. 2017. Nanotechnology in sustainable agriculture: recent developments, challenges, and perspectives. *Frontiers in Microbiology*, **8**: 1014-1026. <https://doi.org/10.3389/fmicb.2017.01014>
- Rawashdeh, R.Y., Harb, A.M., AlHasan, A.M. 2020. Biological interaction levels of zinc oxide nanoparticles; lettuce seeds as case study. *Heliyon*, **6**: 1-10. <https://doi.org/10.1016/j.heliyon.2020.e03983>
- Rekha, K., Nirmala, M., Nair, M.G., Anukaliani, A. 2010. Structural, optical, photocatalytic and antibacterial activity of zinc oxide and manganese doped zinc oxide nanoparticles. *Physica B: Condensed Matter*, **405**: 3180-3185. <https://doi.org/10.1016/j.physb.2010.04.042>
- Rizwan, M., Ali, S., Ali, B., Adrees, M., Arshad, M., Hussain, A., Rehman, M.Z., Waris, A.A. 2019. Zinc and iron oxide nanoparticles improved the plant growth and reduced the oxidative stress and cadmium concentration in wheat. *Chemosphere*, **214**: 269-277. <https://doi.org/10.1016/j.chemosphere.2018.09.120>
- Rosi, N.L., Mirkin, C.A. 2005. Nanostructures in biodiagnostics. *Chemical Reviews*, **105**: 1547-1562. <https://doi.org/10.1021/cr030067f>
- Salavati-Niasari, M., Davar, F., Khansari, A. 2011. Nanosphericals and nanobundles of ZnO: synthesis and characterization. *Journal of Alloys and Compounds*, **509**: 61-65. <https://doi.org/10.1016/j.jallcom.2010.08.060>
- Seyedi, N., Koyama, M., Mackins, C.J., Levi, R. 2002. Ischemia promotes renin activation and angiotensin formation in sympathetic nerve terminals isolated from the human heart: contribution to carrier-mediated norepinephrine release. *Journal of Pharmacology and Experimental Therapeutics*, **302**: 539-544. <https://doi.org/10.1124/jpet.302.2.539>
- Yang, K., Wang, X., Zhu, L., Xing, B. 2006. Competitive sorption of pyrene, phenanthrene, and naphthalene on multiwalled carbon nanotubes. *Environmental Science & Technology*, **40**: 5804-5810. <https://doi.org/10.1021/es061081n>
- Yusan, S., Bampaiti, A., Aytas, S., Erenturk, S., Aslani, M.A.A. 2016. Synthesis and structural properties of ZnO and diatomite-supported ZnO nanostructures. *Ceramics International*, **42**: 2158-2163. <https://doi.org/10.1016/j.ceramint.2015.09.169>
- Zak, A.K., Razali, R., Abd Majid, W.H., Darroudi, M. 2011. Synthesis and characterization of a narrow size distribution of zinc oxide nanoparticles. *International Journal of Nanomedicine*, **6**: 1399-1403. <https://doi.org/10.2147/IJN.S19693>